CHAPTER IV
RESULTS AND DISCUSSION

4.1 Adsorbent Characterizations

4.1.1 Surface Area Analysis

Activated carbons used in the study were produced from different biomass sources and chemical surface treatment, which inherently affect their ability to adsorb methane and carbon dioxide. Nitrogen adsorption-desorption isotherms of the adsorbents were conducted using an Autosorb-1MP (Quantachrome Instrument). The adsorbents were previously degassed at 300 °C, and the study was carried out at liquid nitrogen temperature, -196 °C. The specific surface area was calculated with the Brunauer, Emmet, and Teller (BET) method, and the pore size distribution was obtained by Dubinin-Astakhov, DA method. The total pore volume was estimated from the adsorption of nitrogen at relative pressure of 0.99. In this study, CSAC and PSAC are referred to coconut shell activated carbon and palm shell activated carbon, respectively.

Table 4.1 BET surface area, micropore volume, and average pore diameter of investigated adsorbents

Adsorbent	Physical Characterization			
	BET surface area (m^2/g)	Micropore volume (cm^3/g)	Total pore volume (cm^3/g)	Average pore diameter (Å)
CSAC – Untreated	909	0.48	0.50	22.0
CSAC – Treated by KOH	941	0.50	0.52	22.2
CSAC – Treated by H_2SO_4	959	0.51	0.53	21.9
PSAC – Untreated	815	0.44	0.46	22.5

Table 4.1 summarizes the BET surface area, total pore volume, micropore volume, and average pore diameter of the adsorbents. The BET surface area of the CSAC is higher than that of the PSAC. After the acid/basic treatment, the surface area increases. It should be noted that the micropore volume, total pore volume, and average pore diameter of the CSAC after treatment regardless of the treatment method are about the same.

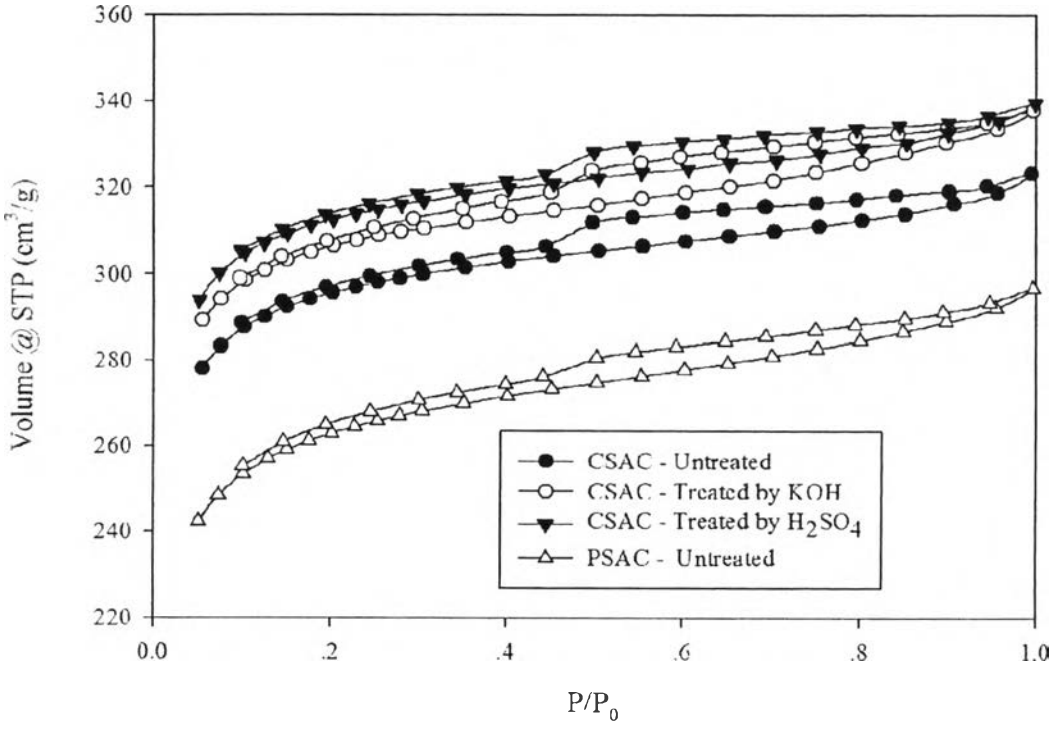

Figure 4.1 Nitrogen adsorption-desorption isotherms of: untreated CSAC, CSAC treated by potassium hydroxide, CSAC treated by sulfuric acid, and untreated PSAC.

Figure 4.1 shows the nitrogen adsorption-desorption isotherms at -196 °C for all adsorbents. The shape of the isotherms shows the characteristics of micropore solid. The hysteresis loop can be seen from the nitrogen adsorption-desorption isotherms. The loop is usually associated to the narrow slit-shaped pores and the evidence of mesoporosity of the adsorbents (Rouquerol *et al.*, 1999).

Figure 4.2 presents the pore size distribution of the adsorbents, where the micropores and mesopores can be observed. All the adsorbents exhibit pores in the range between 10 and 40 Å, being micro and mesopores. It can confirm the hysteresis loops of the nitrogen isotherms due to their small amount of mesopore. It can also be seen that the all of the activated carbons are microporous materials.

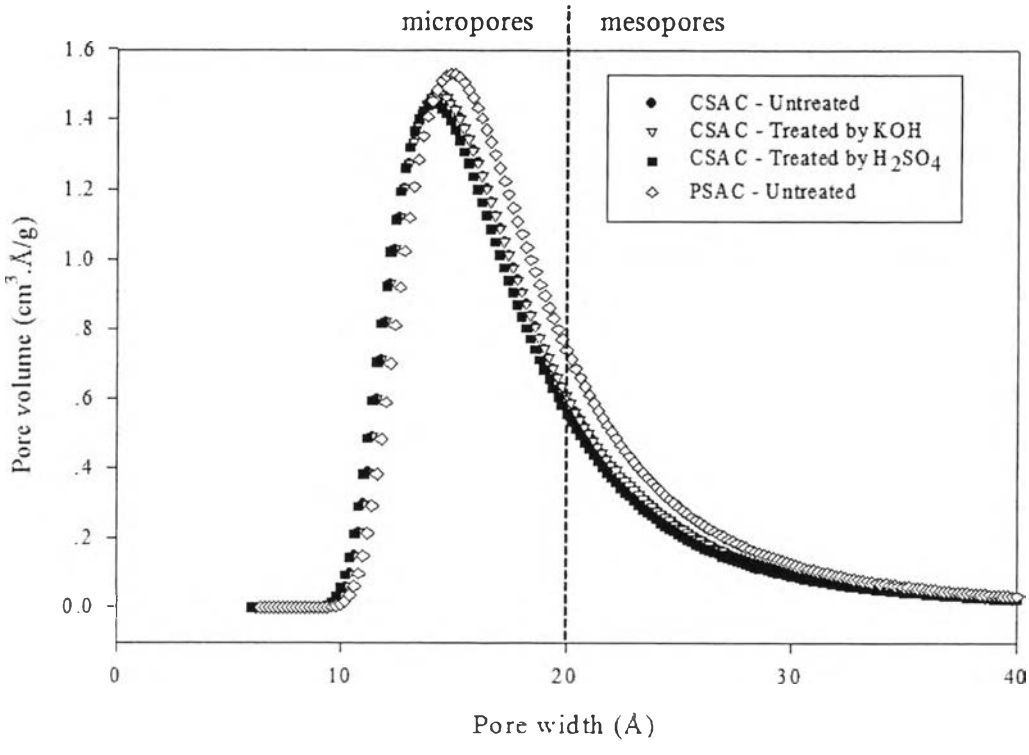

Figure 4.2 Pore size distribution (DA) of: untreated CSAC, CSAC treated by potassium hydroxide, CSAC treated by sulfuric acid, and untreated PSAC.

Alcañiz-Monge *et al.* (1997) and Lozano-Castello *et al.* (2002) reported that the micropore is the size of porosity useful for methane storage applications. Regarding methane adsorption capacity, it is known that a reasonably linear relationship exists between micropore volume and methane uptake. The advanced ANG adsorbent needs to have micropore volume near 50%, solid carbon near 40% and mesopore and macropore volume near 10% (Vasiliev *et al.*, 2000).

4.1.2 Scanning Electron Microscopy

SEM, Hitachi S-4800, was used to investigate the morphology of the CSAC adsorbent with the applied voltage at 2 kV and varying magnifications of 250, 1,000, 1,500, and 10,000 as shown in Figure 4.1.

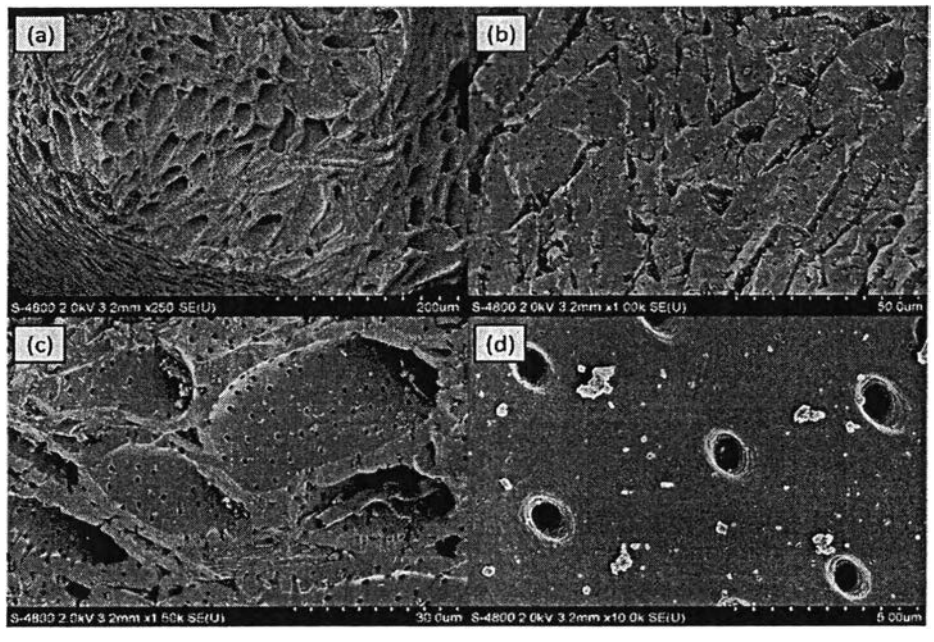

Figure 4.3 SEM micrographs of the CSAC with magnifications of (a) 250, (b) 1,000, (c) 1,500, and (d) 10,000.

Figure 4.3 shows the surface morphologies of the adsorbent from the SEM. Only overall surface and macropores can be observed at these magnifications. The result implies that the CSAC is a high porosity material, which is likely to be suitable as an adsorbent for the ANG storage technology.

4.2 Adsorption Experiments

4.2.1 Single Component Adsorption

Investigation on the adsorption kinetics of methane and carbon dioxide was carried out in a stainless steel packed bed column with an inside diameter of 7.0 mm at atmospheric pressure and room temperature. Methane and carbon dioxide

composition were varied from 75 to 85 and 5 to 20 vol%, respectively. The breakthrough curves of methane and carbon dioxide were plotted in terms of concentration ratio versus time, as shown in Figures 4.4 and 4.5.

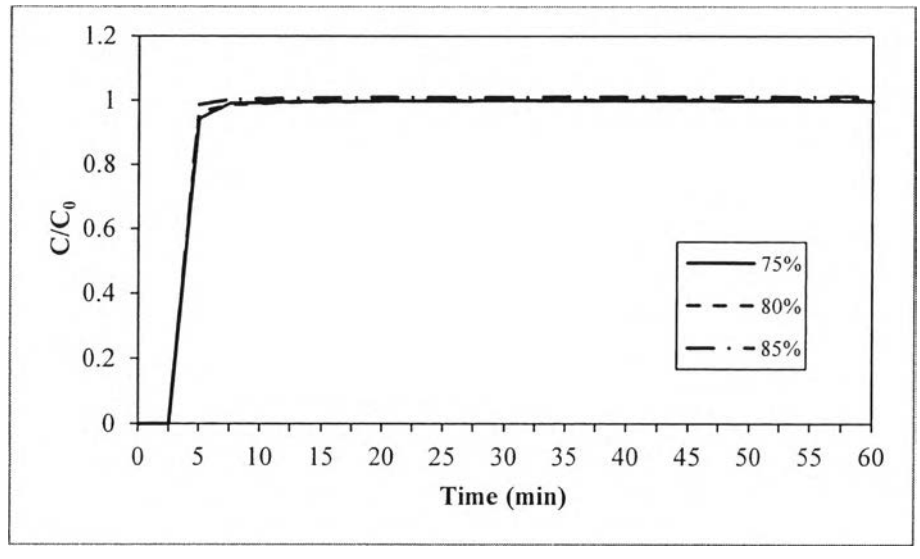

Figure 4.4 Breakthrough curves of methane from the adsorption on the CSAC with the initial concentration of methane at 75, 80, and 85 vol% at room temperature.

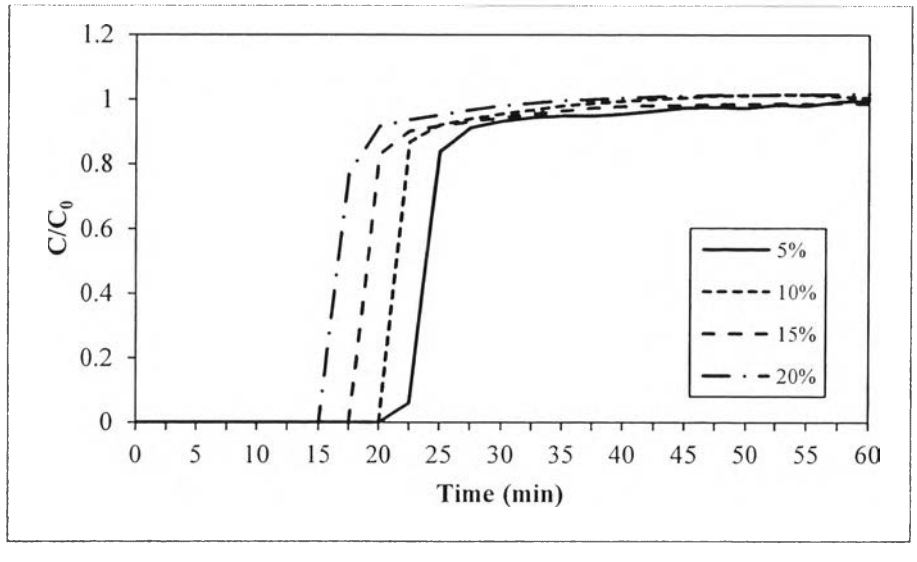

Figure 4.5 Breakthrough curves of carbon dioxide from the adsorption on the CSAC with the initial concentration of carbon dioxide at 5, 10, 15, and 20 vol% at room temperature.

From the methane adsorption, the result shows that the change in the methane concentration from 75 to 85 vol% does not affect the adsorption of methane on the CSAC. In contrast with the carbon dioxide adsorption, the change in its concentration from 5 to 20 vol% significantly affects the adsorption. It can also be seen that, when the concentration of carbon dioxide is increased from 5 to 20 vol%, the eluted time decreases from approximately 20 to 15 min due to faster saturation on the CSAC.

4.2.2 Competitive Adsorption

Methane composition was fixed at 10 vol% and carbon dioxide composition was varied from 10 to 30 vol%. The breakthrough curves of methane and carbon dioxide were plotted in terms of concentration ratio versus time, as shown in Figures 4.6 to 4.11.

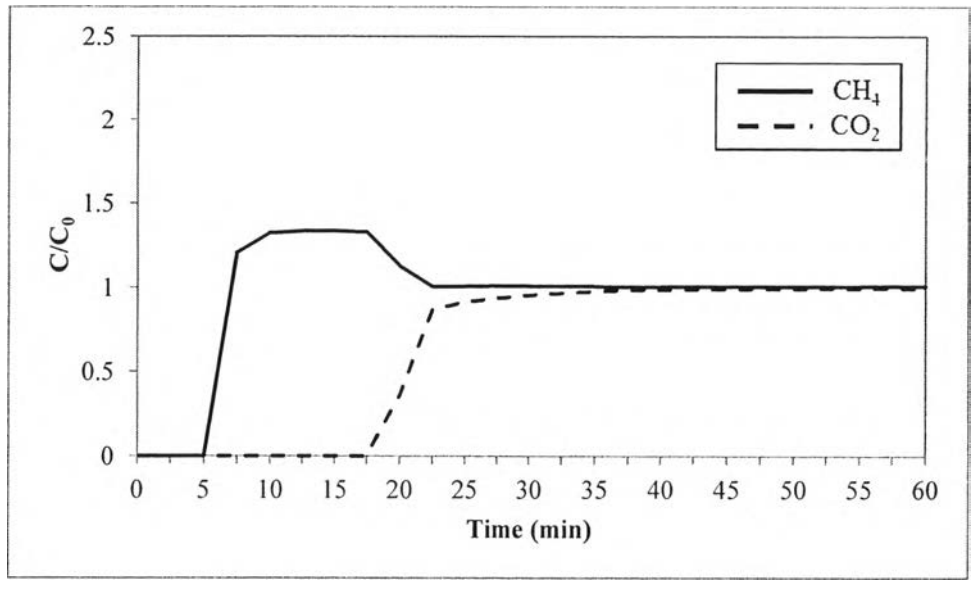

Figure 4.6 Breakthrough curves of methane and carbon dioxide from the competitive adsorption on the CSAC with the initial concentration of methane at 10 vol% and carbon dioxide at 10 vol% at room temperature.

From Figure 4.6, it can be seen that methane breaks through first at about 5 min, followed by carbon dioxide at approximately 17.5 min. Methane roll up can be observed. The roll up reaches the highest concentration ratio at 1.34 before it reverts to the feed concentration at about 22.5 min. The roll up is commonly observed because of the displacement of a relatively weakly adsorbed component on the CSAC, methane, by a more strongly adsorbed component, carbon dioxide.

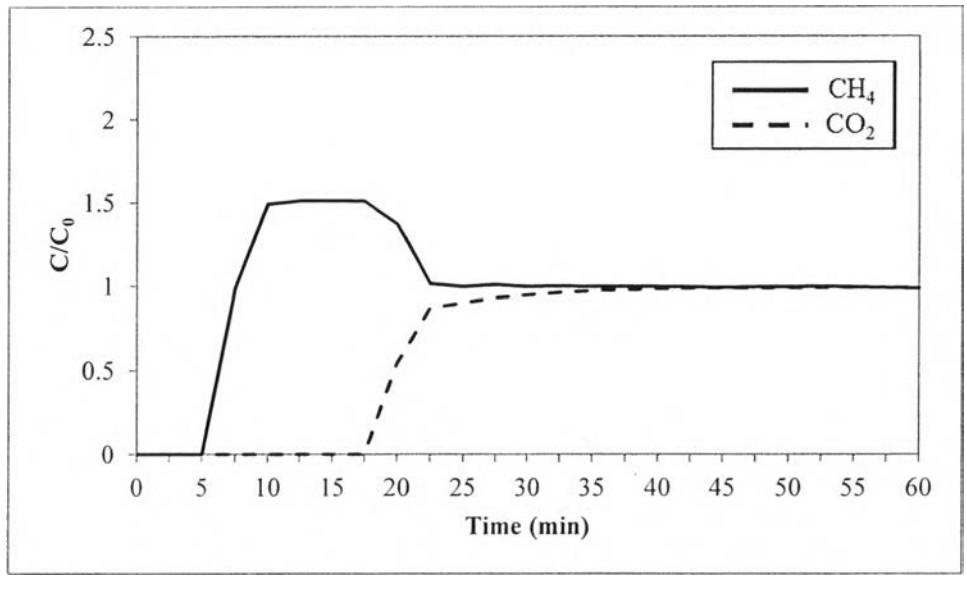

Figure 4.7 Breakthrough curves of methane and carbon dioxide from the competitive adsorption on the CSAC with the initial concentration of methane at 10 vol% and carbon dioxide at 15 vol% at room temperature.

When the carbon dioxide concentration is increased from 10 to 15 vol%, similar adsorption of the two components can be observed, as shown in Figure 4.7. The only difference is on the roll up. Here, the roll up reaches the highest concentration ratio at 1.51, which is higher than that from 10 vol% carbon dioxide. It is because the higher concentration of more strongly adsorbed component, carbon dioxide, results in the greater displacement of weakly adsorbed component, methane.

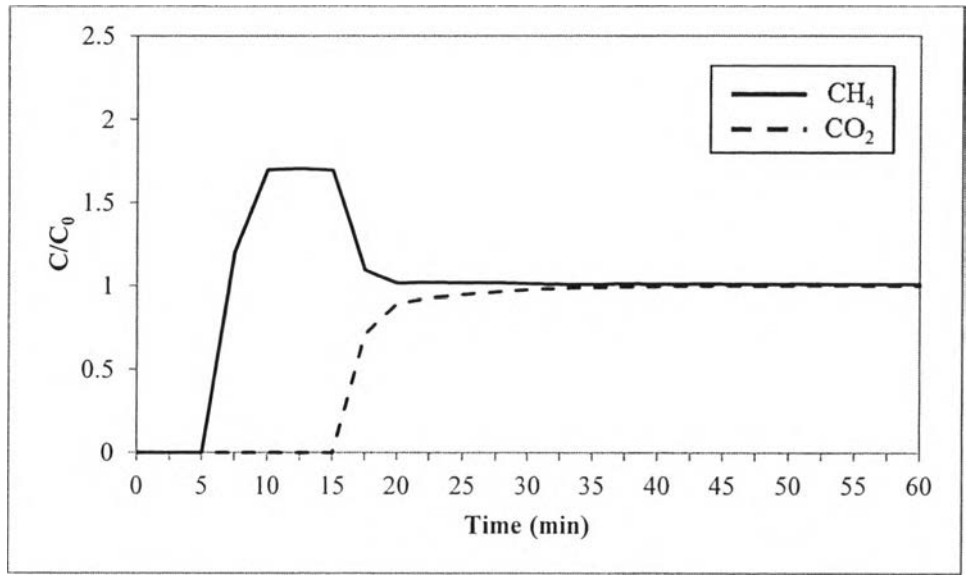

Figure 4.8 Breakthrough curves of methane and carbon dioxide from the competitive adsorption on the CSAC with the initial concentration of methane at 10 vol% and carbon dioxide at 20 vol% at room temperature.

Figure 4.8 shows the breakthrough of methane and carbon dioxide with the initial concentration of 10 and 20 vol%, respectively. From the figure, carbon dioxide breaks through at approximately 15 min, which is faster than that of 10 and 15 vol% carbon dioxide (Figures 4.6 and 4.7) due to its higher concentration that gives shorter time to saturate the adsorbent surface than the low carbon dioxide concentration. The roll up reaches the highest concentration ratio at 1.71 before it reverts to the feed concentration at about 17.5 min, which is also faster than that of low carbon dioxide concentration. That is because, when carbon dioxide begins to break through, some methane is re-adsorbed and its gas phase concentration reverts to that of the feed indicating that the bed is saturated with respect to methane.

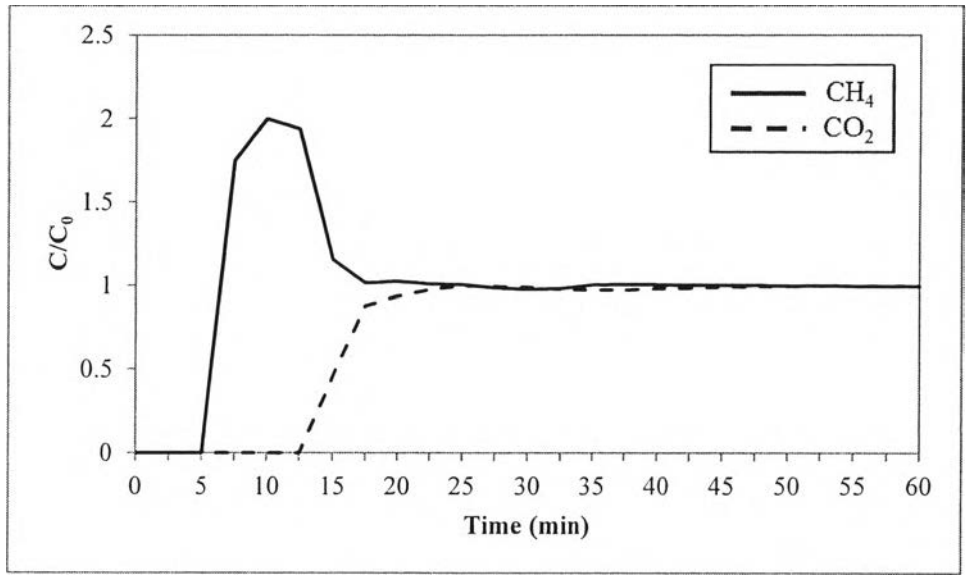

Figure 4.9 Breakthrough curves of methane and carbon dioxide from the competitive adsorption on the CSAC with the initial concentration of methane at 10 vol% and carbon dioxide at 25 vol% at room temperature.

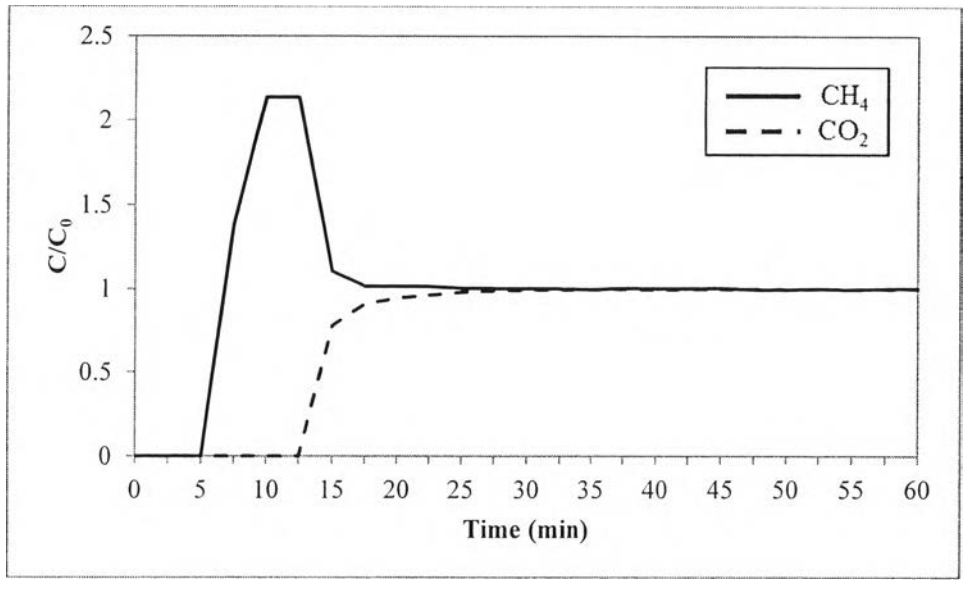

Figure 4.10 Breakthrough curves of methane and carbon dioxide from the competitive adsorption on the CSAC with the initial concentration of methane at 10 vol% and carbon dioxide at 30 vol% at room temperature.

When the carbon dioxide concentration is further increased to 25 and 30 vol%, the decrease in the carbon dioxide breakthrough time from 15 to 12.5 min can be observed, as shown in Figures 4.9 and 4.10. The methane roll up also reaches higher concentration ratio with the increase in the carbon dioxide concentration. Again, this is because the higher concentration of more strongly adsorbed component, carbon dioxide, results in the greater displacement of weakly adsorbed component, methane.

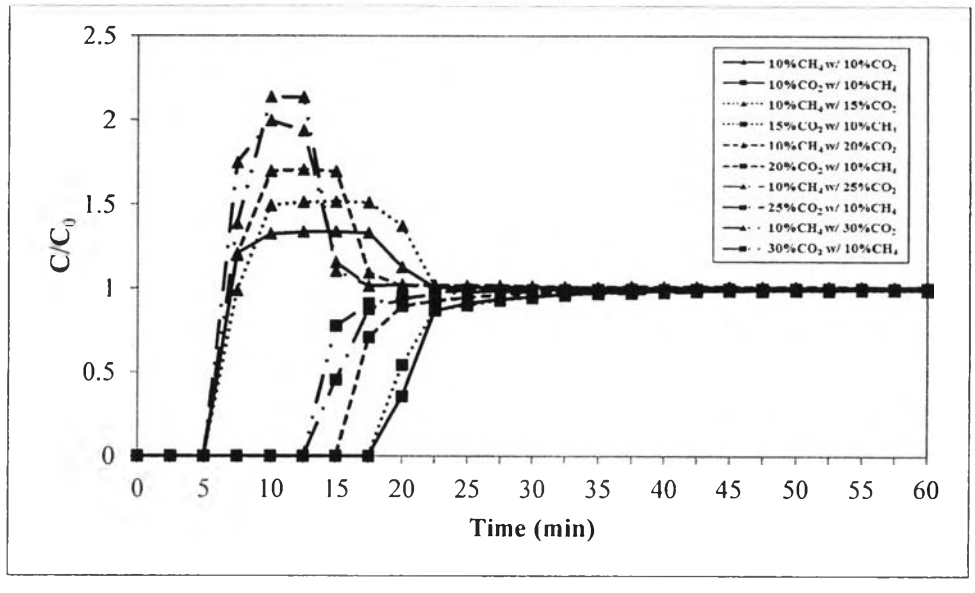

Figure 4.11 Breakthrough curves of methane and carbon dioxide from the competitive adsorption on the CSAC with the initial concentration of methane at 10 vol% and carbon dioxide at 10, 15, 20, 25, and 30 vol% at room temperature.

From Figure 4.11, the weakly adsorbed component, methane, breaks through first at about 5 min. Some of methane is displaced from the adsorbent to give a higher gas phase concentration than was originally present in the feed. As carbon dioxide then begins to break through, some methane is re-adsorbed and its gas phase concentration reverts to that of the feed indicating that the bed is saturated with respect to methane. The displacement of a relatively weakly adsorbed component, methane, by a more strongly adsorbed component, carbon dioxide, is sometimes referred to a roll up effect. In other words, methane roll up increases from the

methane concentration ratio of 1.34 to 2.14 with the increase in the concentration of carbon dioxide from 10 to 30 vol%. It can be seen that carbon dioxide more strongly and selectively adsorbs on the activated carbon than methane. It is because the lower surface diffusivity of carbon dioxide is associated with its higher affinity towards the carbon surface. The adsorbed methane molecule has smaller energy barrier than carbon dioxide does, and this could be due to the quadrupole moment of carbon dioxide compared to the non-polar nature of the methane molecule (Prasetyo and Do, 1998).

4.2.3 Adsorbent Stability

The adsorbent stability was studied by the 3-cycle adsorption-desorption process of methane and carbon dioxide on the investigated adsorbent at atmospheric pressure and room temperature, as shown in Figures 4.12 to 4.21.

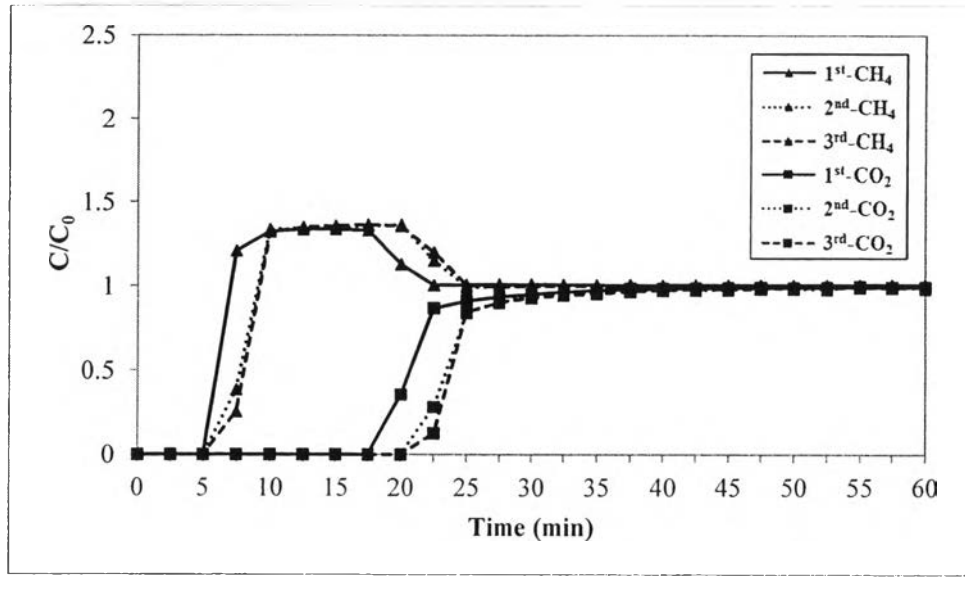

Figure 4.12 Breakthrough curves of methane and carbon dioxide from the 3-cycle adsorption process on the CSAC with the initial concentration of methane at 10 vol% and carbon dioxide at 10 vol% at room temperature.

From the 3-cycle adsorption on the CSAC as shown in Figure 4.12, it can be seen that the breakthrough curves of methane and carbon dioxide is shifted to longer time, and the breakthrough time of carbon dioxide is also increased from 17.5 to 20 min after the first adsorption. This may be because the adsorbed carbon dioxide molecules, which preferentially adsorb on the CSAC, result in the change of the adsorbent surface properties. Hence, the ability of the adsorbent to adsorb gases is decreased after the first adsorption.

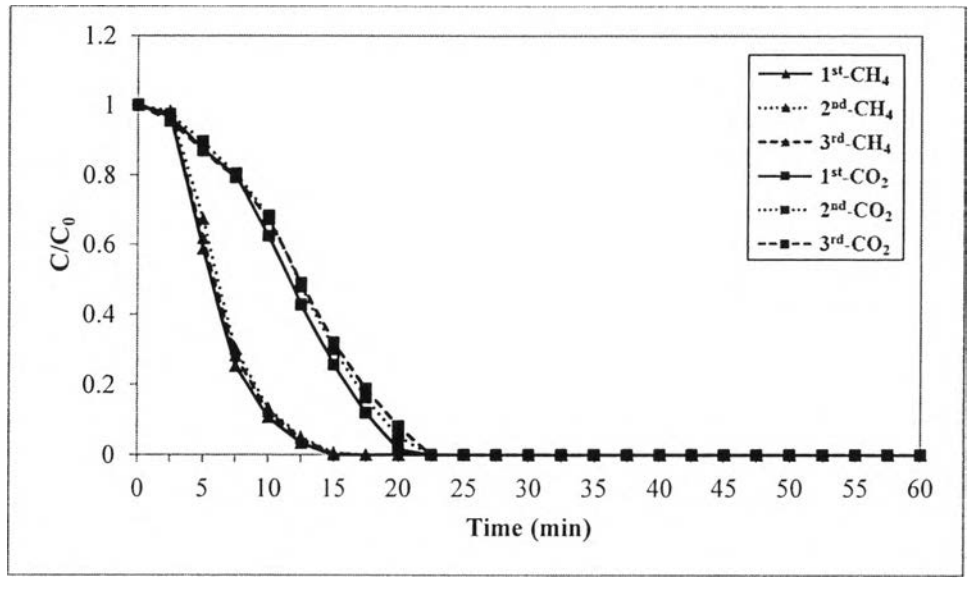

Figure 4.13 Three desorption cycles of methane and carbon dioxide from the CSAC with the initial concentration of methane at 10 vol% and carbon dioxide at 10 vol% at room temperature.

Three desorption cycles of methane and carbon dioxide from the CSAC was also studied. The result from Figure 4.13 exhibits that the change in the desorption cycle from 1 to 3 times does not significantly affect the desorption of methane and carbon dioxide on the CSAC. When the desorption of methane and carbon dioxide was separately considered, it seems that methane always rapidly decreases in its concentration unlike carbon dioxide that slowly decreases in its concentration at longer time compared to methane. This implies that carbon dioxide has stronger interaction with the activated carbon surface than methane. Again, that

is because the polar nature of carbon dioxide, which preferentially adsorbs on the hydrophilic surface of the adsorbent more than the non-polar nature of methane.

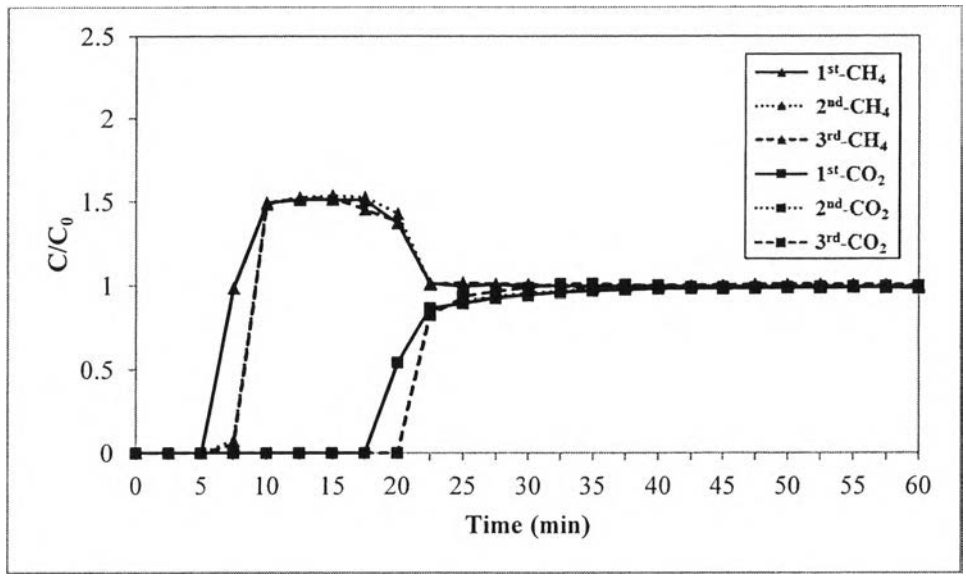

Figure 4.14 Breakthrough curves of methane and carbon dioxide from the 3-cycle adsorption process on the CSAC with the initial concentration of methane at 10 vol% and carbon dioxide at 15 vol% at room temperature.

When the initial concentration of carbon dioxide is increased from 10 to 15 vol%, the similar adsorption of the two components can be observed, as shown in Figure 4.14. The difference is on the breakthrough curves of methane and carbon dioxide and the carbon dioxide breakthrough time, which is changed from 17.5 to 20 min after the first adsorption cycle.

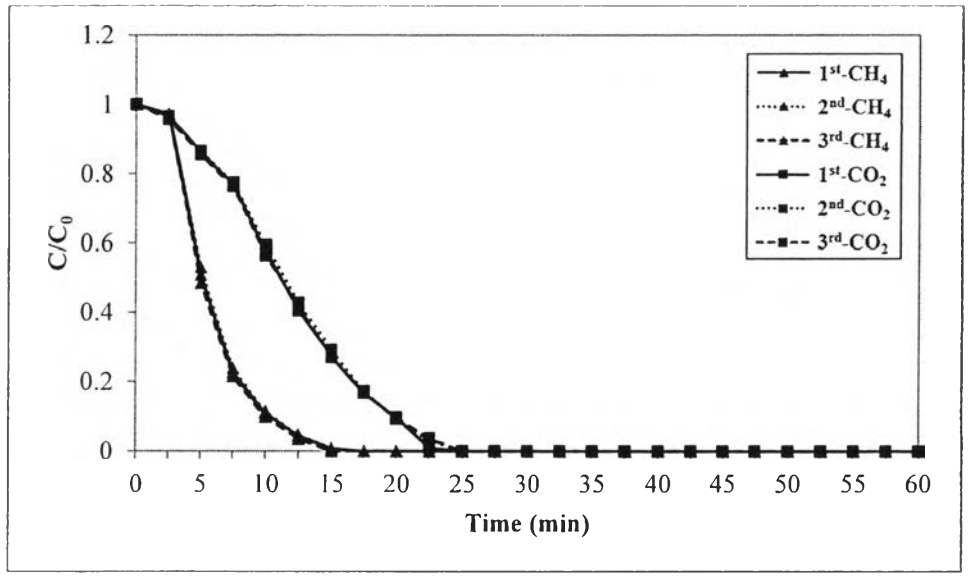

Figure 4.15 Three desorption cycles of methane and carbon dioxide from the CSAC with the initial concentration of methane at 10 vol% and carbon dioxide at 15 vol% at room temperature.

Figure 4.15 displays the alike desorption of the two gases over the 3-cycle desorption. Methane concentration decreases faster than carbon dioxide concentration due to methane is weakly adsorbed on the activated carbon resulting in its shorter time to displace from the adsorbent surface.

Figures 4.16 and 4.17 exhibit the 3-cycle adsorption-desorption of methane and carbon dioxide from the CSAC with the initial concentration of 10 and 20 vol%, respectively. From Figure 4.16, carbon dioxide breaks through at approximately 15 min in the fisrt adsorption cycle, which is faster than that of 10 and 15 vol% carbon dioxide (Figures 4.12 and 4.14). Later, the breakthrough curves of both components and the breakthrough times are shifted to longer time as the number of the adsorption cycle increases from 1 to 3 cycles. And for the desorption, it stays nearly the same throughout the 3-cycle of methane and carbon dioxide desorption on the CSAC, Figures 4.13 and 4.15.

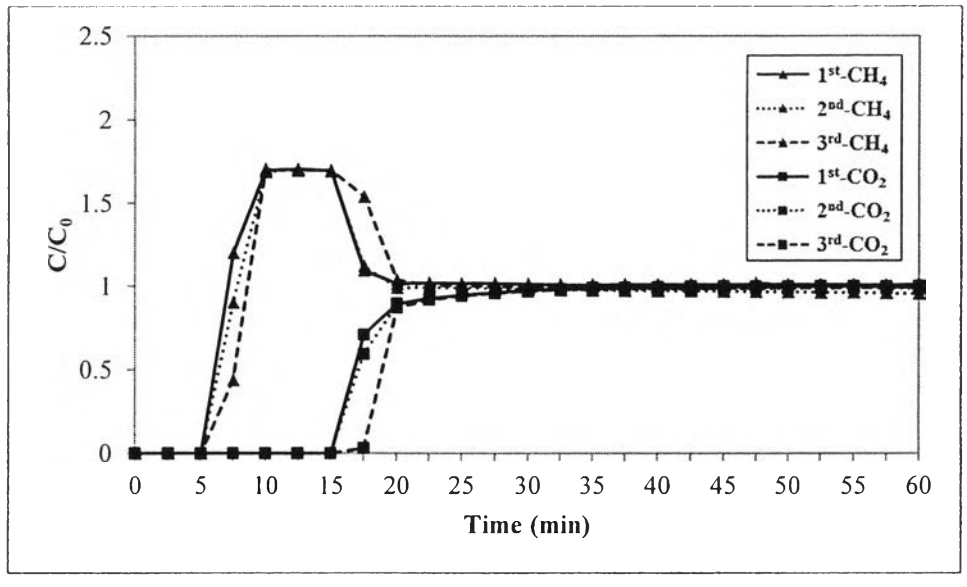

Figure 4.16 Breakthrough curves of methane and carbon dioxide from the 3-cycle adsorption process on the CSAC with the initial concentration of methane at 10 vol% and carbon dioxide at 20 vol% at room temperature.

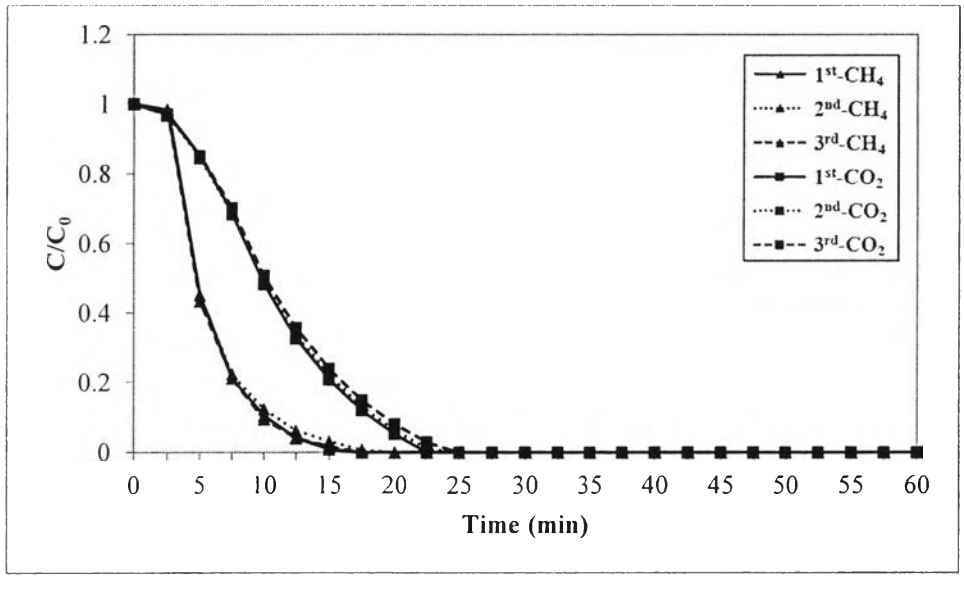

Figure 4.17 Three desorption cycles of methane and carbon dioxide from the CSAC with the initial concentration of methane at 10 vol% and carbon dioxide at 20 vol% at room temperature.

In the same way as in Figures 4.18 to 4.21, when the initial concentration of carbon dioxide is further increased to 25 and 30 vol%, the carbon dioxide breakthrough time of the first adsorption cycle decreases from 15 to 12.5 min. After that, in the next two desorption cycles, the breakthrough curves of methane and carbon dioxide slightly shift to longer time compared to its primary breakthrough curve of the first adsorption cycle. For the breakthrough time of carbon dioxide in Figure 4.20, it can be seen that the breakthrough time of the third adsorption cycle increases to 15 min. Once again, the desorption stays the same throughout the 3-cycle illustrating that the desorption ability of methane and carbon dioxide on the CSAC is not affected within the three cycles.

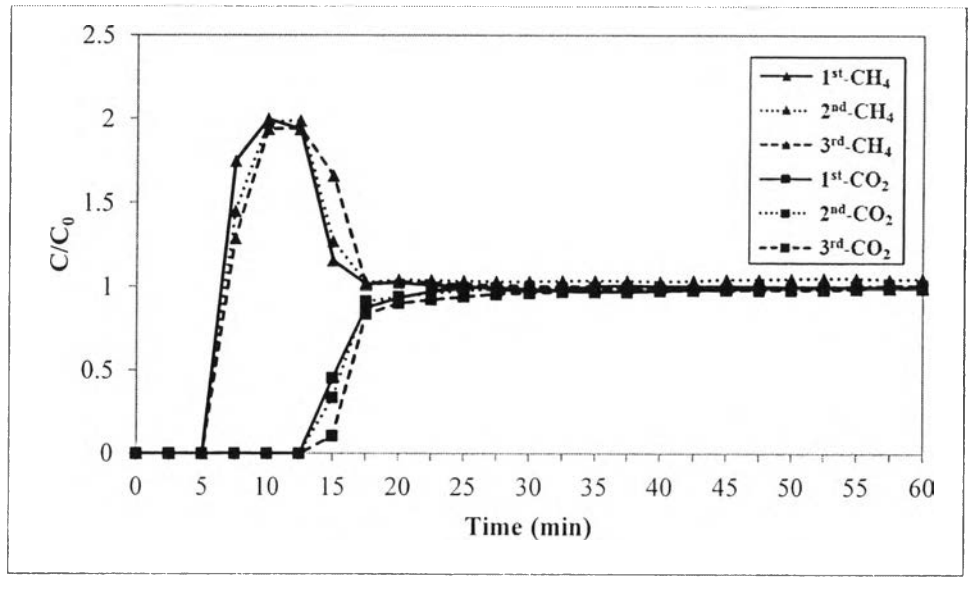

Figure 4.18 Breakthrough curves of methane and carbon dioxide from the 3-cycle adsorption process on the CSAC with the initial concentration of methane at 10 vol% and carbon dioxide at 25 vol% at room temperature.

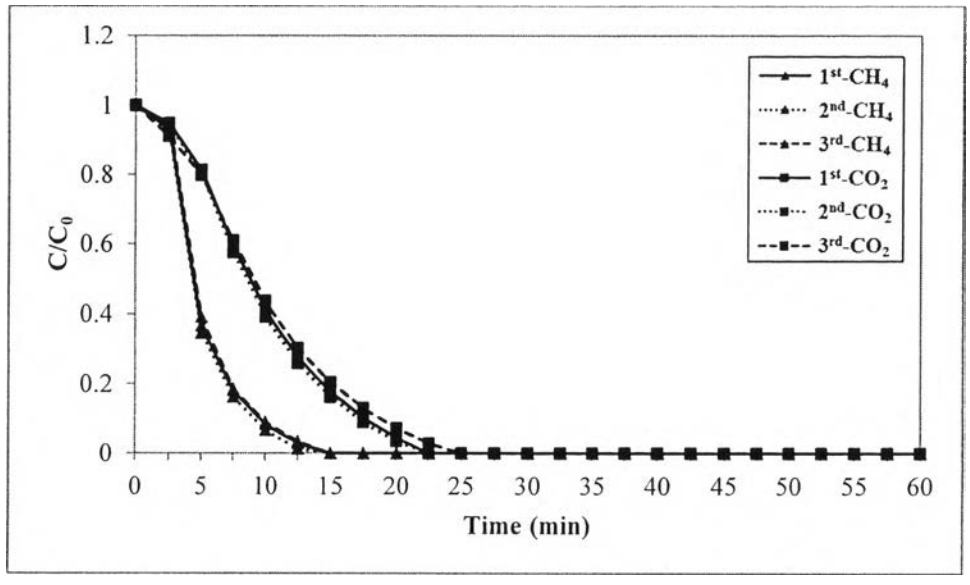

Figure 4.19 Three desorption cycles of methane and carbon dioxide from the CSAC with the initial concentration of methane at 10 vol% and carbon dioxide at 25 vol% at room temperature.

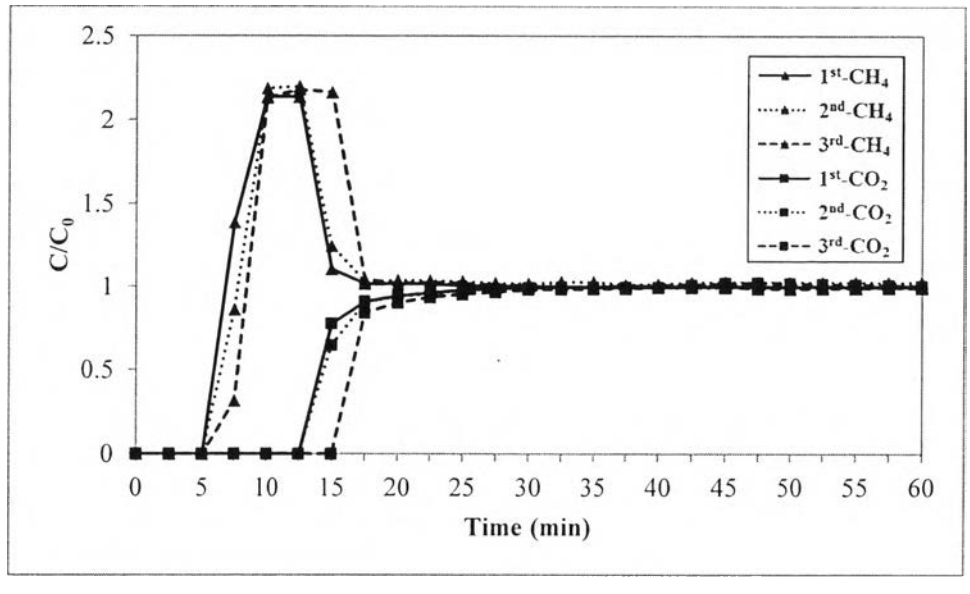

Figure 4.20 Breakthrough curves of methane and carbon dioxide from the 3-cycle adsorption process on the CSAC with the initial concentration of methane at 10 vol% and carbon dioxide at 30 vol% at room temperature.

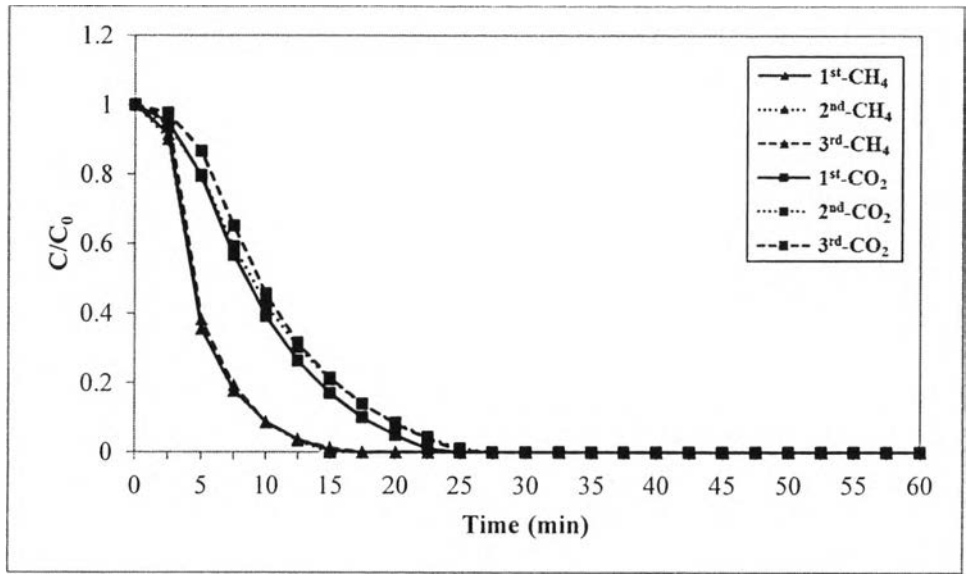

Figure 4.21 Three desorption cycles of methane and carbon dioxide from the CSAC with the initial concentration of methane at 10 vol% and carbon dioxide at 30 vol% at room temperature.

The three adsorption-desorption cycles of methane and carbon dioxide from the CSAC are shown in Figures 4.12 to 4.21. In general, the adsorption of methane and carbon dioxide only changes slightly when the adsorption and desorption is repeated. The breakthrough times of methane and carbon dioxide increase due to the adsorbent lost its ability to adsorb gases. It is likely that some gas molecules block the pores and resulting in a longer time to equilibrate its surface. For the desorption, the result, however, shows that the methane and carbon dioxide desorption is barely affected. The desorption stays relatively the same throughout the three cycles.

4.2.4 Comparison of Competitive Adsorption on Different Adsorbents

Various adsorbents including untreated CSAC, CSAC treated by sulfuric acid, CSAC treated by potassium hydroxide, and untreated PSAC were used to study the competitive adsorption of 10 vol% methane and 10 vol% carbon dioxide. The breakthrough curves of methane and carbon dioxide were plotted in terms of concentration ratio versus time, as shown in Figures 4.22 to 4.26.

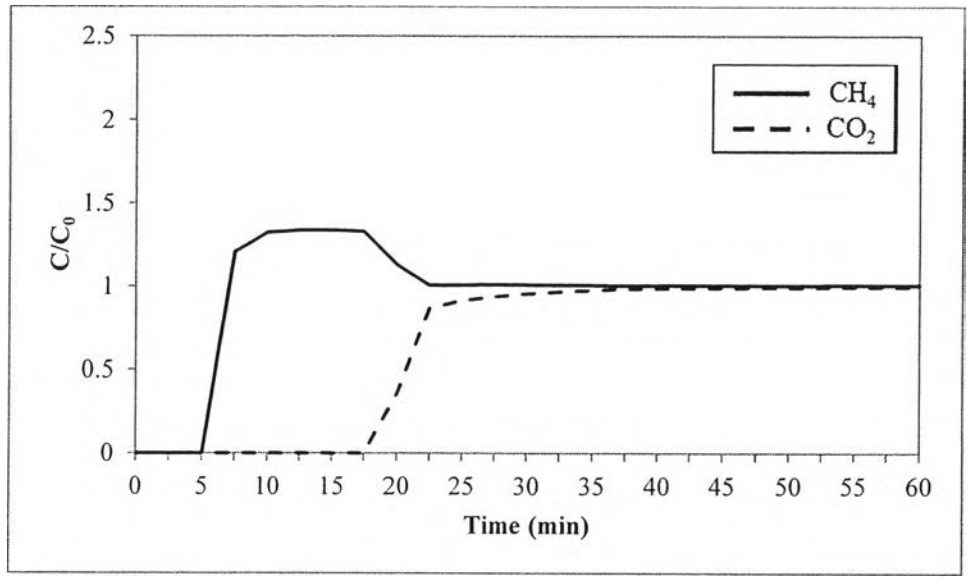

Figure 4.22 Breakthrough curves of methane and carbon dioxide from the competitive adsorption on the untreated CSAC with the initial concentration of methane at 10 vol% and carbon dioxide at 10 vol% at room temperature.

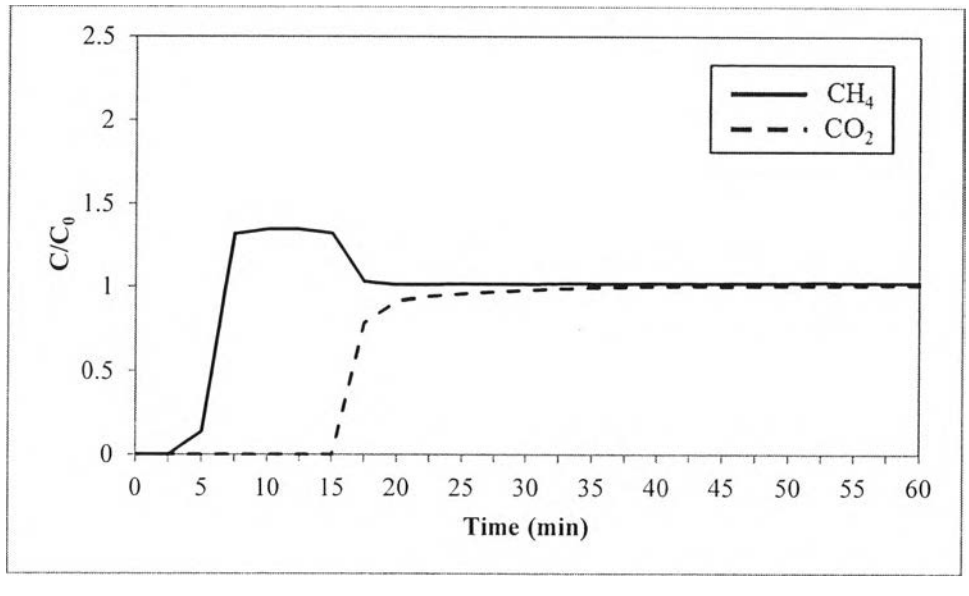

Figure 4.23 Breakthrough curves of methane and carbon dioxide from the competitive adsorption on the CSAC treated by sulfuric acid with the initial concentration of methane at 10 vol% and carbon dioxide at 10 vol% at room temperature.

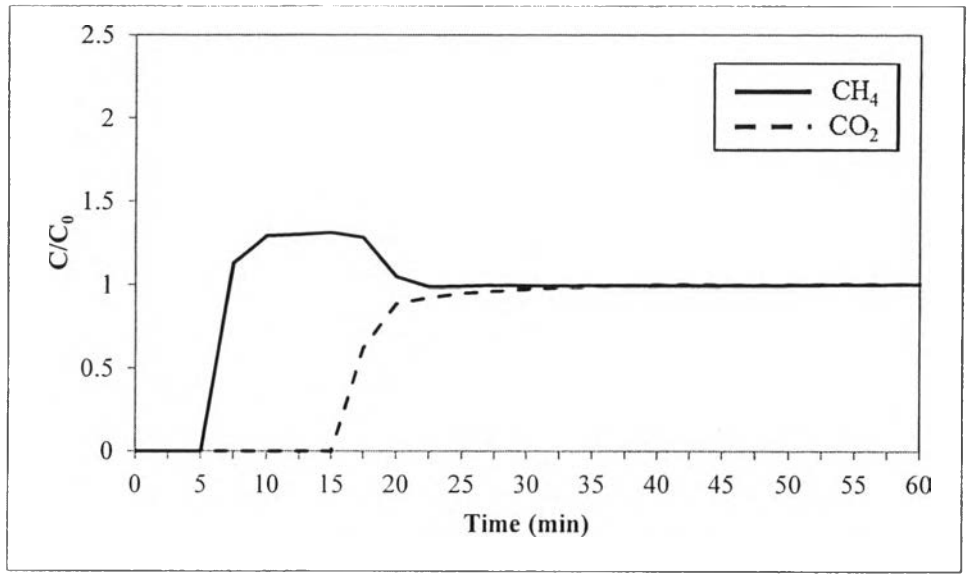

Figure 4.24 Breakthrough curves of methane and carbon dioxide from the competitive adsorption on the CSAC treated by potassium hydroxide with the initial concentration of methane at 10 vol% and carbon dioxide at 10 vol% at room temperature.

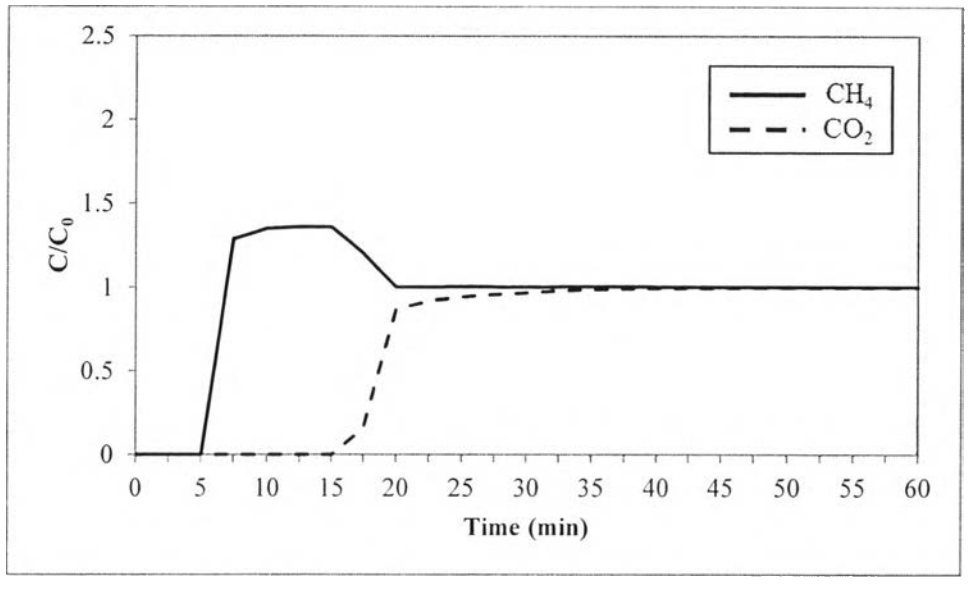

Figure 4.25 Breakthrough curves of methane and carbon dioxide from the competitive adsorption on the untreated PSAC with the initial concentration of methane at 10 vol% and carbon dioxide at 10 vol% at room temperature.

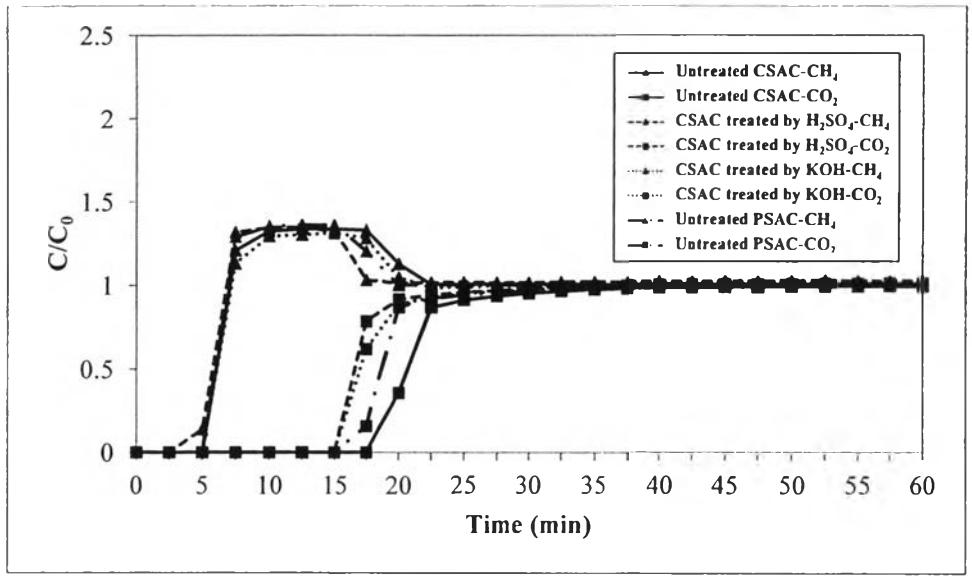

Figure 4.26 Breakthrough curves of methane and carbon dioxide from the competitive adsorption on the untreated CSAC, CSAC treated by sulfuric acid, CSAC treated by potassium hydroxide, and untreated PSAC with the initial concentration of methane at 10 vol% and carbon dioxide at 10 vol% at room temperature.

For detail comparison, all the results from Figures 4.22 to 4.25 were plotted in Figure 4.26. From Figure 4.26, it can be seen that methane breaks through first at about 2.5 min from the CSAC treated by sulfuric acid, followed by the untreated CSAC at about 5 min. Methane elutes from the CSAC treated by potassium hydroxide and untreated PSAC at the same time as that of the untreated CSAC. The methane roll up reaches the highest concentration ratio at approximately 1.3, which is very similar to all adsorbents. The difference in the time, in which the methane concentration reverts to the feed concentration, can be observed for the untreated CSAC, CSAC treated by potassium hydroxide, untreated PSAC, and CSAC treated by sulfuric acid at 22.5, 22.5, 20, and 20 min, respectively. The carbon dioxide breakthrough time is decreased subsequently from the adsorption on the untreated CSAC at 17.5 min to the adsorption on the untreated PSAC, CSAC treated by potassium hydroxide, and CSAC treated by sulfuric acid at approximately 15 min. A possible reason could be that the chemical treatment resulting in shorter time to

equilibrate the adsorbent surface with respect to carbon dioxide. Thus, weakly adsorbed component, methane, may be displaced faster by strongly adsorbed component, carbon dioxide. As a result of the surface treatment method on the CSAC by sulfuric acid and potassium hydroxide, the inorganic or other impurities inside the pore could be removed, and the treatment may also open the active pores leading to the increase in the surface area, as seen in Table 4.1. In 2005, Wu and coworkers studied the development of the activated carbon surface by the chemical activation of activated charcoal with potassium hydroxide. It was found that potassium hydroxide could develop micropores, which can enhance the adsorption of methane and carbon dioxide. Under the alkaline environment, it is expected to have the formation of oxygen functional groups on the surface of activated carbon. Moreover, in 2005, Guo and coworkers studied the chemical activation of activated carbon with sulfuric acid. The PSAC prepared by the use of sulfuric acid as an activating agent suggested their potential applications in gas adsorption by the internal surface area development concept, which causes its relatively large micropore surface area. In 2012, Olivares-Marín and coworkers also studied the surface treatment of activated carbon. The activated carbon from cherry stones was prepared by the method of physical activation in air, followed by the chemical activation in sulfuric acid. It was found that after chemical treatment, sulfuric acid yields the activated carbon with a lower level of inorganic matters. For the untreated PSAC, the difference in physical characteristic properties may result in the shorter breakthrough time of carbon dioxide compared to the untreated CSAC that was carried out in the same condition. From Table 4.1, it can be seen that the untreated PSAC has the BET surface area about 815 m^2/g, which is less than that 909 m^2/g of the untreated CSAC. The untreated PSAC also has less micropore volume and total pore volume, so it may use shorter time to fulfill the adsorption of the feed gas due to its less surface capacity. In fact, the adsorption properties of porous carbon materials are defined not only by the porous structure but also by the presence of surface chemical functionalities that could be different by the nature of the starting materials and the preparation conditions applied. Thus, it is very difficult to describe the behavior of each adsorbed component on different types of adsorbents with only one factor either the physical properties or the chemical properties.

The adsorbent stability was also studied by the 3-cycle adsorption-desorption process of methane and carbon dioxide on the untreated CSAC, CSAC treated by sulfuric acid, CSAC treated by potassium hydroxide, and untreated PSAC at atmospheric pressure and room temperature with the same initial concentration of methane and carbon dioxide at 10 and 10 vol%, respectively. The breakthrough curves and the desorption cycles of methane and carbon dioxide on the investigated adsorbents for the three cycles are shown in Figures 4.27 to 4.34.

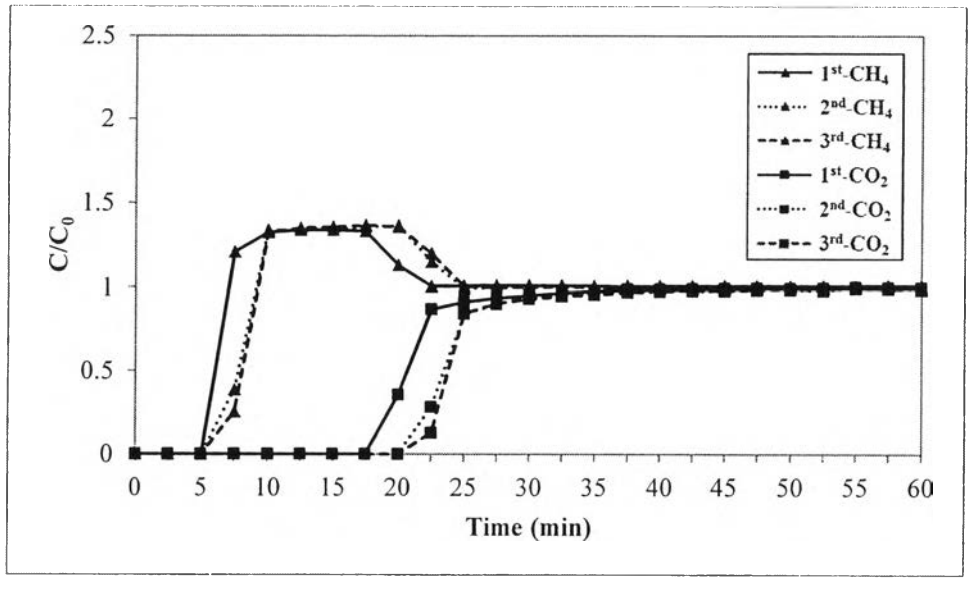

Figure 4.27 Breakthrough curves of methane and carbon dioxide from the 3-cycle adsorption process on the untreated CSAC with the initial concentration of methane at 10 vol% and carbon dioxide at 10 vol% at room temperature.

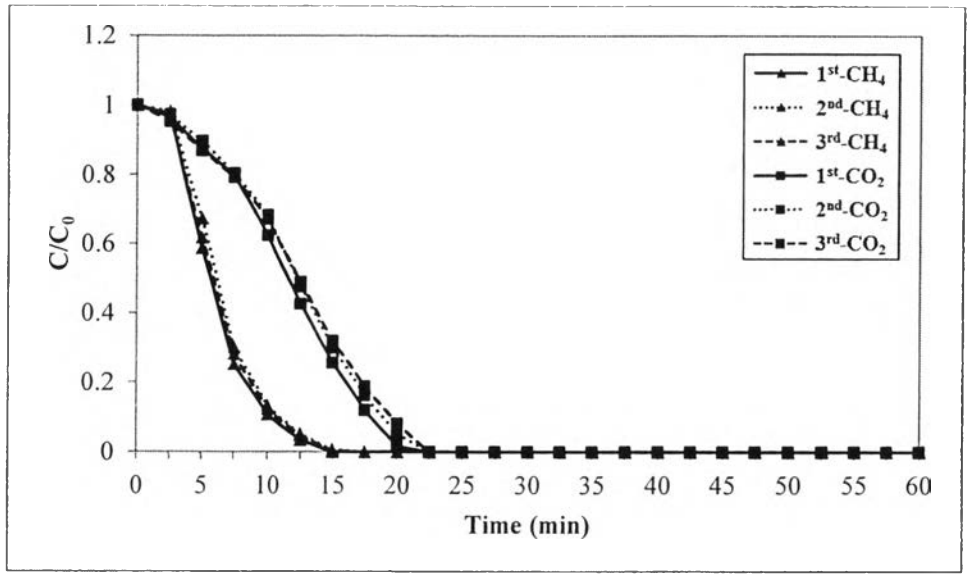

Figure 4.28 Three desorption cycles of methane and carbon dioxide from the untreated CSAC with the initial concentration of methane at 10 vol% and carbon dioxide at 10 vol% at room temperature.

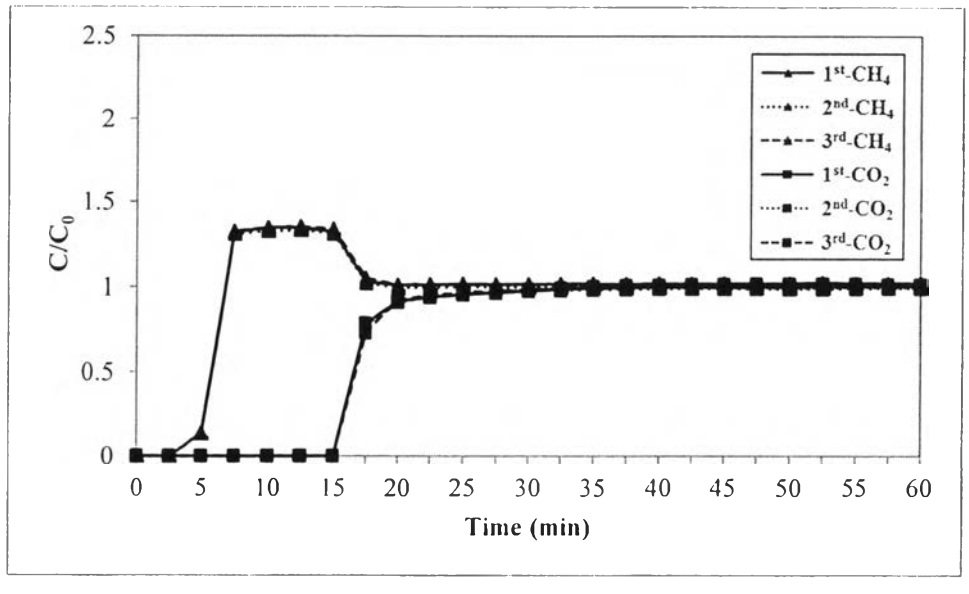

Figure 4.29 Breakthrough curves of methane and carbon dioxide from the 3-cycle adsorption process on the CSAC treated by sulfuric acid with the initial concentration of methane at 10 vol% and carbon dioxide at 10 vol% at room temperature.

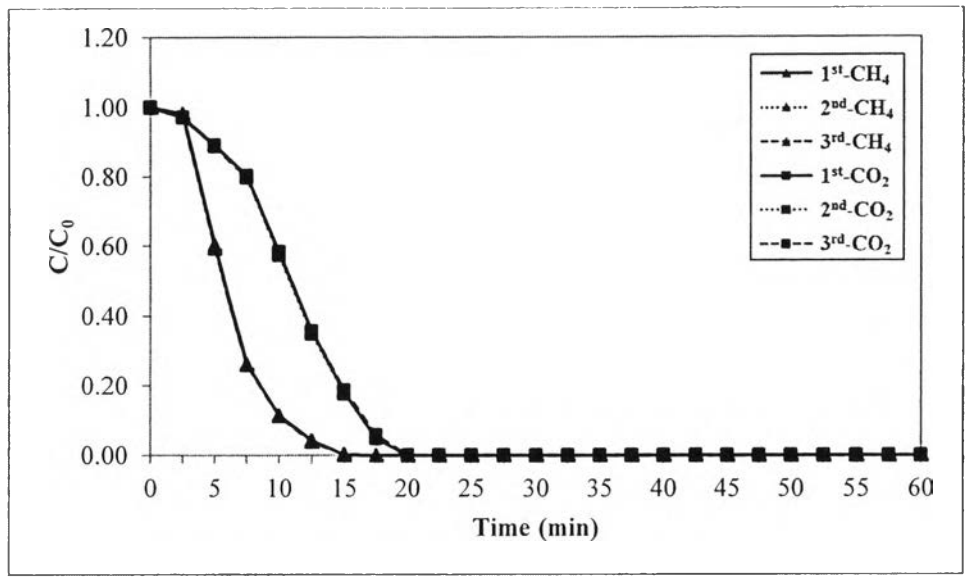

Figure 4.30 Three desorption cycles of methane and carbon dioxide from the CSAC treated by sulfuric acid with the initial concentration of methane at 10 vol% and carbon dioxide at 10 vol% at room temperature.

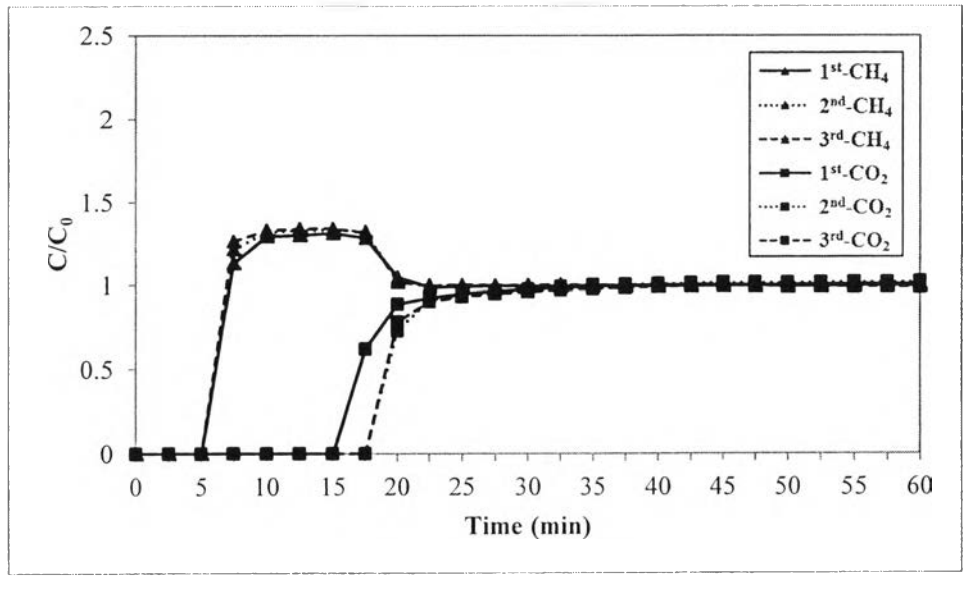

Figure 4.31 Breakthrough curves of methane and carbon dioxide from the 3-cycle adsorption process on the CSAC treated by potassium hydroxide with the initial concentration of methane at 10 vol% and carbon dioxide at 10 vol% at room temperature.

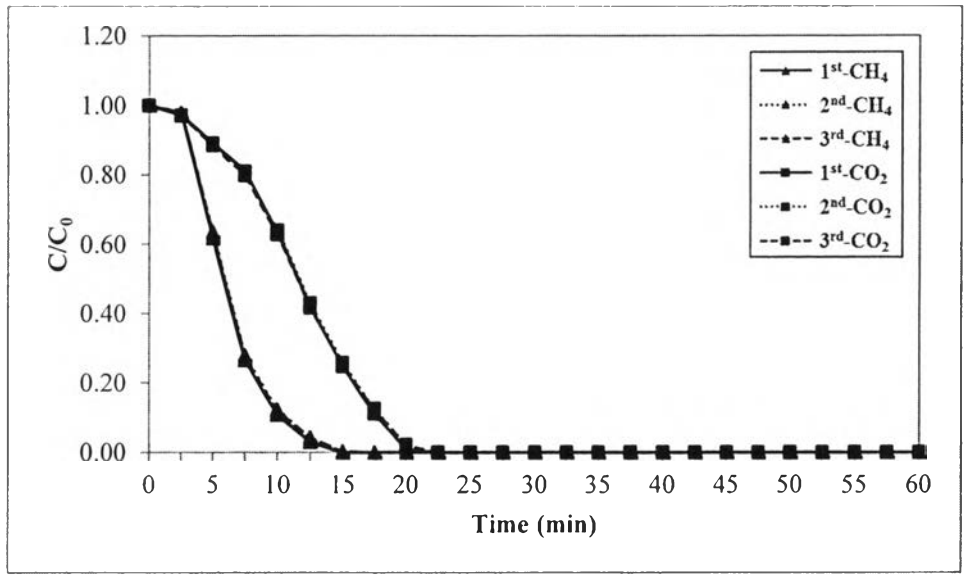

Figure 4.32 Three desorption cycles of methane and carbon dioxide from the CSAC treated by potassium hydroxide with the initial concentration of methane at 10 vol% and carbon dioxide at 10 vol% at room temperature.

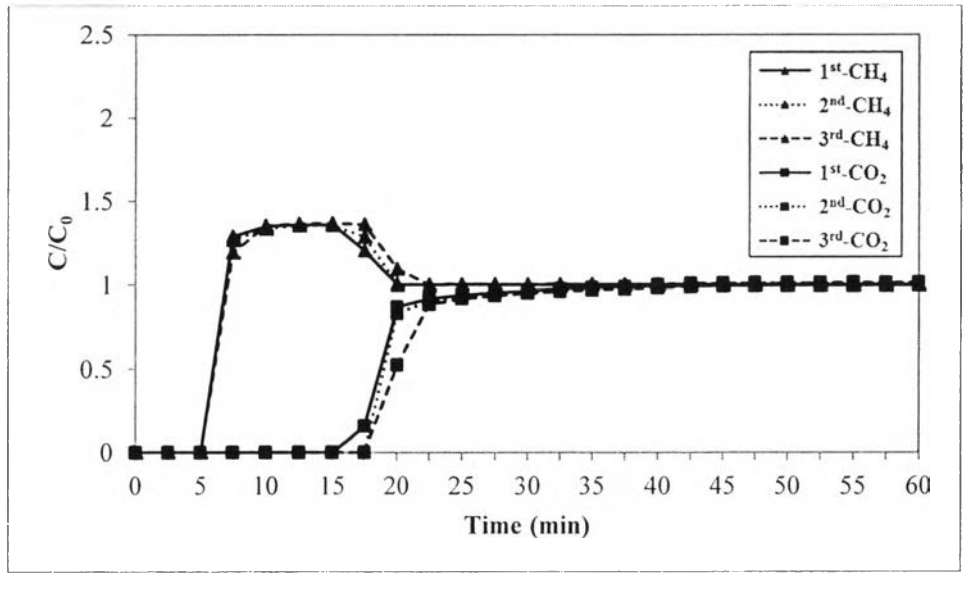

Figure 4.33 Breakthrough curves of methane and carbon dioxide from the 3-cycle adsorption process on the untreated PSAC with the initial concentration of methane at 10 vol% and carbon dioxide at 10 vol% at room temperature.

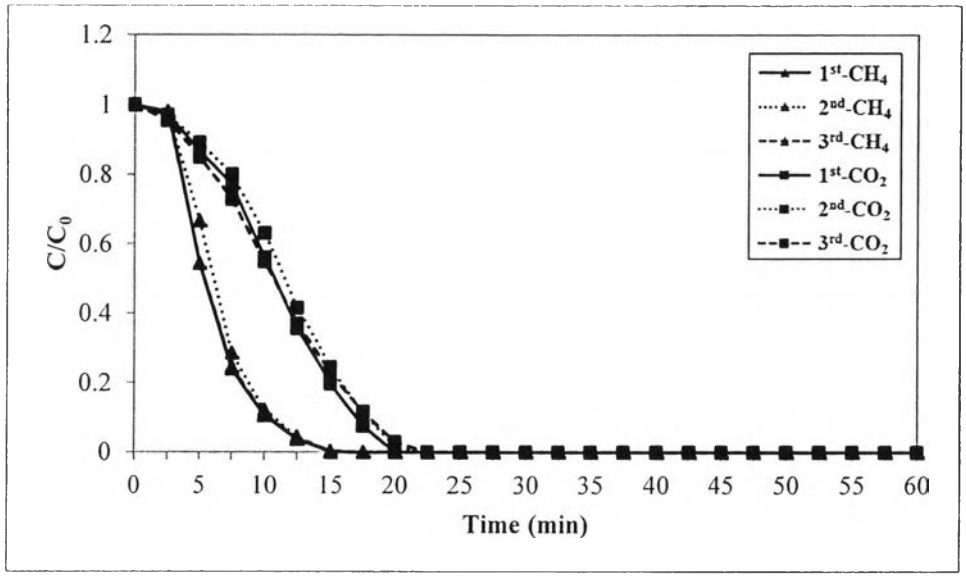

Figure 4.34 Three desorption cycles of methane and carbon dioxide from the untreated PSAC with the initial concentration of methane at 10 vol% and carbon dioxide at 10 vol% at room temperature.

From the 3-cycle adsorption, the breakthrough curves of methane and carbon dioxide from the regenerated adsorbents shows the same breakthrough patterns for all adsorbents. The results show that the adsorbent stability of the untreated CSAC, CSAC treated by potassium hydroxide, and untreated PSAC is only slightly affected when the adsorption cycle is increased. The breakthrough times of methane and carbon dioxide increase due to the adsorbent lost its ability to adsorb gases. Some gas molecules block the pores and resulting in a longer time to equilibrate its surface. Another reason may be because the adsorbed carbon dioxide molecules, which preferentially adsorb on all the adsorbents result in the change of the adsorbent surface properties. In contrast, the stability of the CSAC treated by sulfuric acid is hardly affected with the increase in the adsorption cycle, as seen in Figure 4.29. It has no difference in the breakthrough curves and the breakthrough times of both gases during its regeneration cycles. This could be due to its cleaner surface after the treatment that allows the feed gas molecules to adsorb and desorb easily. It is likely that no gas molecules remain and block the active pores after the regeneration cycles. In addition, to the desorption, the methane and carbon dioxide

desorption are barely affected. The desorption stays relatively the same throughout the 3-cycle for all adsorbents.

Back to the results that were observed in this study, all adsorbents including the untreated CSAC, CSAC treated by sulfuric acid, CSAC treated by potassium hydroxide, and untreated PSAC preferentially adsorb carbon dioxide than methane. The adsorbed methane molecules are replaced by the adsorption of carbon dioxide indicating the decrease in the adsorption capacity of methane. Hence, in the presence of carbon dioxide, these adsorbents may not be suitable to be used as a material for the ANG storage technology. On the contrary, when a point of view of the carbon dioxide and methane separation is considered instead of the ANG technology, these adsorbents show the performance in the separation competent. A series of the breakthrough experiments demonstrated that the ability to selectively adsorb carbon dioxide from the binary mixtures was high due to the adsorption capacity of carbon dioxide is much higher than that of methane.